Central European Journal of Energetic Materials
ISSN 1733-7178; e-ISSN 2353-1843
Copyright © 2017 Institute of Industrial Organic Chemistry, Poland

Cent. Eur. J. Energ. Mater. 2017, *14*(2): 361-374 DOI: 10.22211/cejem/68392

Temperature-dependent Shock Initiation of CL-20-based High Explosives

Zhengdi Pi, Lang Chen,* Junying Wu

State Key Laboratory of Explosion Science and Technology, Beijing Institute of Technology, Beijing 100081, China
**E-mail: chenlang@bit.edu.cn*

Abstract: To investigate the effects of temperature on the shock initiation characteristics of hexanitrohexaazaisowurtzitane (CL-20), shock initiation experiments on heated C-1 explosive (94% epsilon phase CL-20, and 6% binder, by weight) were performed at temperatures of 20 °C, 48 °C, 75 °C, 95 °C, 125 °C, 142 °C, and 175 °C. An explosive driven flyer device was used to initiate the C-1 charges and manganin pressure gauges were embedded in the C-1 specimen to record the pressure changes with time. Our results show that C-1 becomes more sensitive as the temperature is increased from 20 °C to 95 °C. The ε to γ phase transition in CL-20 occurs at 125 °C; C-1 with CL-20 in the γ phase at 142 °C is less shock sensitive than C-1 with CL-20 in the ε phase at 95 °C or 75 °C. Compared with C-1 at 142 °C, C-1 at 175 °C shows a dramatic increase in shock sensitivity. An ignition and growth reactive flow model was used to simulate the shock initiation of C-1 at various temperatures, and the parameters were obtained by fitting the experimental data. With this parameter set, the shock initiation characteristics of C-1 for temperatures between 20 °C and 175 °C can be derived.

Keywords: CL-20, shock initiation, heated explosive, phase transitions, numerical simulation

1 Introduction

CL-20, or hexanitrohexaazaisowurtzitane, is a high-energy and highly sensitive explosive [1, 2]. The sensitivity of CL-20-based explosives to a single stimulus such as shock, impact, or heat, is well documented. However, hazardous scenarios usually involve multiple stimuli, such as heating to relatively high temperatures followed by fragment impact, which produce a shock in the hot

explosive material [3]. Therefore, investigating the effect of temperature on the shock sensitivity of CL-20 is important for explosive design and safety analysis; moreover, the temperature-dependent shock initiation characteristics of CL-20 have not been thoroughly studied. Previous investigations have shown that increasing the temperature of explosive materials affects their shock sensitivity in two ways: by an increase in the porosity, which is attributed to thermal expansion [4], and by transformation of polymorphs that occurs at higher temperatures, a phase transition that can lead to a change in shock sensitivity [5].

There are four polymorphs for CL-20 (α, β, γ, and ε) at ambient temperature and atmospheric pressure, the ε phase being reported to be the most stable phase of CL-20 under ambient conditions [6, 7]. Gump [8] found that the *epsilon* phase is stable under ambient pressure to a temperature of 120 °C and a phase transition to the *gamma* phase occurs at 125 °C. The *gamma* phase remains stable until thermal decomposition occurs above 150 °C. Thus, thermal expansion and polymorph transformation in a ε-CL-20-based explosive, C-1 (94% *epsilon* phase CL-20, and 6% binder, by weight), which are caused by increased temperature, may both affect the shock sensitivity of C-1.

In the present work, we carried out experiments to investigate the influence of temperature on the shock sensitivity of C-1. An explosive driven flyer device was used to initiate the unconfined C-1 charges at various temperatures. The explosive specimen was uniformly heated by heating plates and a heating jacket. Thermocouples were used to monitor the temperature distribution in the specimen during the heating process, and the temperature change in the C-1 target was used to judge whether polymorphic transformation had occurred. The pressure in the C-1 specimen was recorded at several distances from the impact surface by manganin pressure gauges embedded in the specimen. An ignition and growth reactive flow model was used to simulate the shock initiation of the C-1 explosive, and the relationship between the reactive rate parameters and the temperature was established. These coefficients were then used to calculate the initial shock pressure-distance to detonation relationship (Pop-plots) for the C-1 explosive at different temperatures.

2 Geometries of the Shock Initiation Experiments

The configuration for the unconfined, heated C-1 shock initiation experimental apparatus is shown in Figure 1. Two heating plates were placed symmetrically on the aluminum buffer plate to heat the upper surface of the C-1 specimen while the bottom of the specimen was heated by the heating plates embedded in the base plate. Additionally, a semi-open heating jacket, whose inner diameter was

Copyright © 2017 Institute of Industrial Organic Chemistry, Poland

slightly bigger than the diameter of the explosive column, was placed around the specimen, and radiation heating was applied on the sides of the specimen. This heating method ensured that the temperature was uniformly distributed in the C-1 explosive column. The polytetrafluoroethylene (PTFE) buffer plate, steel flyer plate, and PTFE support play an important role in preventing heat transfer to the booster explosive, maintaining the properties of the booster explosive constant during the heating process. When the final desired temperature of the C-1 specimen had been reached, the explosive plane-wave lens was detonated by the detonator, a high-pressure plane detonation wave was generated by the plane-wave lens and booster explosive, and then attenuated by the PTFE buffer plate. As the plane shock wave propagates through the steel flyer plate, the plate begins to move downwards. When the steel flyer plate strikes the aluminum buffer plate, it generates a planar shock wave and begins the initiation process of the C-1 target. The intensity of the initial shock pressure can be adjusted by changing the thickness of the PTFE and the aluminum buffer plate.

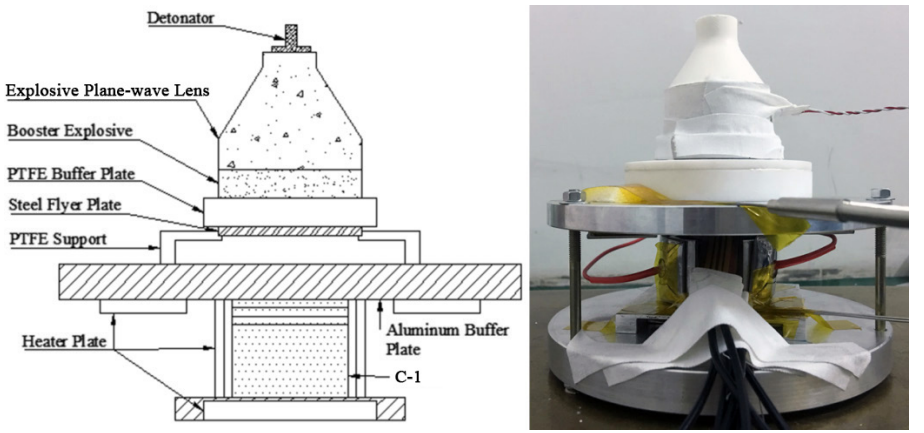

Figure 1. Schematic drawing and photograph of the shock initiation experimental apparatus

The detailed parameters of the shock initiation device are as follows: the diameter of the plane-wave lens was 50 mm; the TNT booster explosive was 10 mm thick with a 50 mm diameter; the PTFE buffer plate was 10 mm thick with a 60 mm diameter; the flyer plate was composed of 3-mm-thick steel with a 50 mm diameter. The C-1 explosive specimens were pressed discs, 40 mm in diameter and with various thicknesses (1 mm, 2 mm, 3 mm, and 25 mm), and with an average density of 1.91 g/cm^3. To assemble the C-1 target specimen, the 25-mm-thick disc was placed at the bottom of the apparatus and a groove

Copyright © 2017 Institute of Industrial Organic Chemistry, Poland

was carved into the upper surface of the disc. A 0.5-mm-diameter thermocouple was placed in the groove to monitor the internal temperature of the specimen during the heating process (Figure 2a). The three thin discs were then placed on the top of the 25 mm disc, and then four manganin piezoresistive pressure gauges were embedded between the discs. The gauges were coated with 100-μm-thick Teflon® insulation on both sides to prevent electrical conduction between the gauges when the material becomes reactive. The disc assembly is shown in Figure 2b. This experimental configuration allows the measurement of the pressure histories at several distances from the impact surface.

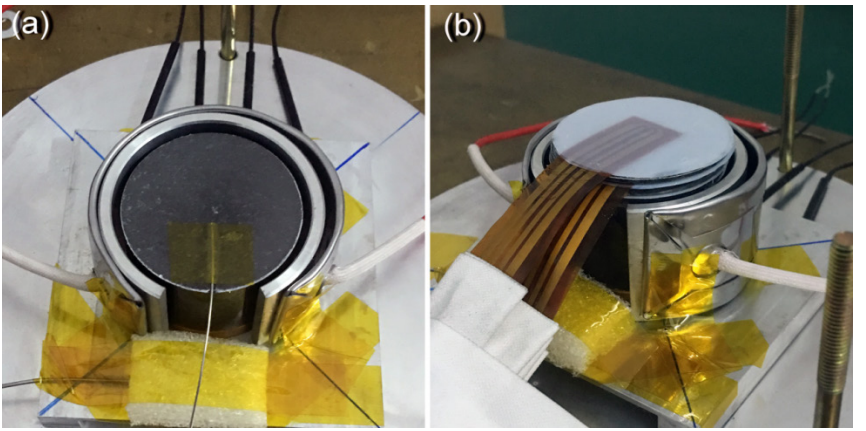

Figure 2. Photograph of the 25 mm C-1 specimen surrounded by the heating jacket (a) and the four assembled discs with the pressure gauges (b)

3 Preheating Experiments

To determine the temperature distribution in the explosive specimen and whether the ε→γ phase transformation of CL-20 occurs, preheating experiments were carried out on the C-1 discs. Two thermocouples were used to monitor the temperatures of the aluminum buffer plate and the C-1 specimen. Figure 3 shows the temperatures recorded by the two thermocouples as the temperature of the C-1 discs was raised to 142 °C. The temperature of the aluminum buffer plate quickly reached the final desired temperature and remained stable. The temperature of the C-1 discs rose rapidly up to about 120 °C, then slowed until about 130 °C, followed by a steady temperature rise until 142 °C. Previous studies showed that ε-CL-20 remains stable up to 120 °C, and then transforms into the γ phase at 125 °C [8, 9]. Thus, the bend in the temperature profile around

Copyright © 2017 Institute of Industrial Organic Chemistry, Poland

125 °C indicates this phase transition. We therefore concluded that at 142 °C, the ε→γ phase transition in the C-1 specimen was complete.

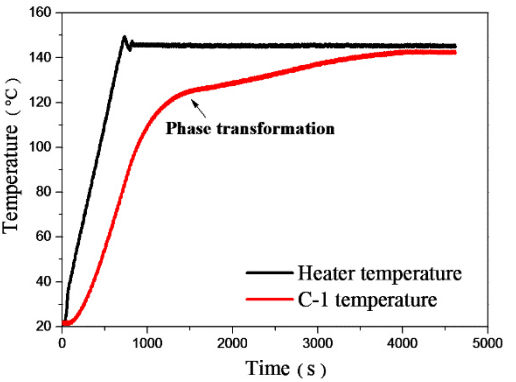

Figure 3. Thermal profiles of the heating plate and the C-1 specimen as the specimen was heated to 142 °C

Fourteen shock initiation experiments on the heated C-1 explosive specimens were performed at temperatures of 20 °C, 48 °C, 75 °C, 95 °C, 125 °C, 142 °C, and 175 °C, respectively. To investigate the influence of the temperature on the shock sensitivity of C-1, all of the shock initiation experiments, apart from the two at ambient temperature, had the same loading conditions. In these experiments, C-1 was heated to the final desired temperature and held at that temperature for the time needed to ensure that the heat was evenly distributed throughout the specimen.

4 Results and Discussion

Figure 4a shows the pressure histories for the 20 °C C-1 discs, with shock initiated at an input pressure of 3.57 GPa. The pressure gauges were placed on top of the specimen and between the discs. All of the pressure profiles show a flattening of the curve after the initial rise, and then a small increase in amplitude behind the shock front, indicating that a small reaction had occurred in the specimen. When the C-1 specimens were heated to 48 °C and 75 °C, and subjected to the same shock load, the increased temperature accelerated the reaction rate of the C-1 explosive. Figure 4b shows the pressure histories measured by the four pressure gauges for 95 °C C-1, with shock initiated at an input pressure of 3.61 GPa. The reaction energy effectively supports the shock wave at a depth of 5 mm, with the pressure at the shock front reaching about 33 GPa.

Copyright © 2017 Institute of Industrial Organic Chemistry, Poland

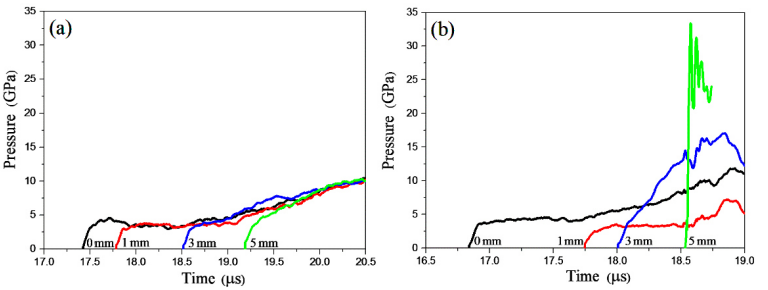

Figure 4. Pressure profiles recorded by the four pressure gauges for the C-1 specimen; the shock was initiated at the same loading conditions (a) 20 °C, 3.57 GPa, (b) 95 °C, 3.61 GPa

These results indicated that under the same loading conditions, the shock sensitivity of C-1 increases as the temperature is increased from 20 °C to 95 °C. Figure 4 also demonstrates that the initial shock pressures are almost unchanged as the specimen temperature is increased, because the coefficient of thermal expansion for the ε phase of CL-20 is relatively small [8], and the shock impedance of C-1 is almost unchanged in this temperature range. Thus, a small part of the increased sensitivity may be attributed to the increased porosity at higher temperatures, which results in more hot-spot ignition sites under shock compression. The increased sensitivity may also be attributed to a more rapid growth of these reacting hot spots, because the chemical decomposition is propagating in hotter C-1 material [4, 5, 10].

As the temperature was increased from 95 °C to 125 °C, the rate of pressure increase did not increase, but decreased. Because 125 °C is the critical temperature of the ε→γ solid phase transition for CL-20, CL-20 may not be fully converted from the ε to γ phase at this temperature. To investigate the shock sensitivity characteristic of CL-20 after the ε→γ transition, the C-1 specimen was heated to 142 °C and shock initiated at an input pressure of 2.91 GPa; the pressure histories are shown in Figure 5a. As the temperature rose from 95 °C to 125 °C and 142 °C, under the same loading conditions, the initial shock pressure decreased from 3.61 GPa to 3.33 GPa, and 2.91 GPa, respectively. This indicates a polymorphic transformation of CL-20 from the ε to γ phase, which leads to a 6% volume increase [11]. The phase transformation leads to a decrease in the specimen density and creates new voids, creating more hot spots under shock compression; however, compared with 125 °C, 95 °C, and even 75 °C, the shock to detonation of C-1 slows down at 142 °C. Therefore, the C-1 specimen of CL-20 in the γ phase at 142 °C is less shock sensitive than C-1 of CL-20 in the ε phase at 95 °C or 75 °C.

Copyright © 2017 Institute of Industrial Organic Chemistry, Poland

Figure 5b shows the pressure histories measured by the four pressure gauges for 175 °C C-1. The run distance to detonation for 175 °C C-1 is approximately 4 mm, much shorter than the run distance for 142 °C C-1, which is about 7 mm. Thus, we conclude that after the CL-20 polymorphic transformation from the ε to the γ phase is complete, as the temperature is increased further, the shock sensitivity of C-1 increases again.

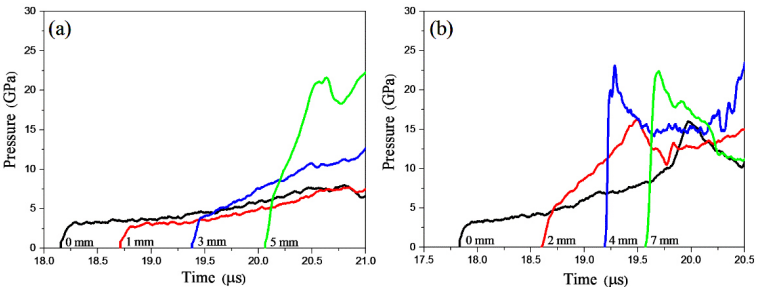

Figure 5. Pressure profiles recorded by the four pressure gauges for the C-1 specimen; the shock was initiated at the same loading conditions (a) 142 °C, 2.91 GPa, (b) 175 °C, 2.98 GPa

5 Numerical Simulation

The explosive shock initiation numerical model was established to simulate the shock initiation experiments. The specimen size and shock initiation conditions in the simulation model were the same as in the experiments. According to the symmetry of the testing device, a two-dimensional axisymmetric model was used in the simulation. The exact details of each shock initiation experiment were replicated in the model using 20 zones per millimeter in the explosive specimen and the Teflon® coated manganin pressure gauges. The calculated pressure history in the center of each gauge set was compared with the measured pressure history. The shock initiation process leading to detonation was simulated using a nonlinear finite element method [12].

A high explosive burn model and the equation of state (EOS) in the JWL (Jones-Wilkins-Lee) form [13] were used in modelling TNT and explosive 8701 (an RDX-based explosive) with an explosive plane-wave lens and booster explosive. The parameters for TNT and 8701 are shown in Table 1, where ρ_0 is the initial density, D is the shock velocity and p_{cj} is the shock pressure at the Chapman-Jouguet state.

Copyright © 2017 Institute of Industrial Organic Chemistry, Poland

Table 1. Parameters for TNT and 8701 explosive

Explosive	ρ_0 [g·cm^{-3}]	D [cm·μs^{-1}]	p_{cj} [Mbar]	A [Mbar]	B [Mbar]	R_1	R_2	ω	E_0 [Mbar]
8701	1.70	0.8315	0.295	8.545	0.2049	4.60	1.35	0.25	0.085
TNT	1.64	0.6930	0.270	3.713	0.0323	4.15	0.95	0.30	0.070

The PTFE buffer plate, aluminum buffer plate, and steel flyer plate were modelled as elastic plastic hydro material using the EOS in the Gruneisen form. The Gruneisen parameters for the inert materials are listed in Table 2.

Table 2. Gruneisen parameters for the inert materials

Inert materials	ρ_0 [g·cm^{-3}]	C [mm·μs^{-1}]	S_1	S_2	S_3	γ_0	a
PTFE	2.15	1.68	1.123	3.983	-5.797	0.59	0.0
Steel	7.83	4.57	1.49	0.0	0.0	1.93	0.5
Aluminum	2.7	5.24	1.4	0.0	0.0	1.97	0.48

The ignition and growth reactive flow model [14] was used to simulate the shock initiation of the C-1 explosive. Two JWL equations of state were used in this reactive flow model, one for the unreacted explosive and another for the reaction products:

$$P_e = Ae^{-R_1 v_e} + Be^{-R_2 v_e} + \frac{\omega C_v T_0}{v_e} \tag{1}$$

$$P_p = Ae^{-R_1 v_p} + Be^{-R_2 v_p} + \frac{\omega C_v T_p}{v_p} \tag{2}$$

where v_e and T_0 are the relative volume and temperature, respectively, of the unreacted explosive; v_p and T_p are the relative volume and temperature, respectively, of the reaction products; P_e and P_p are the initial pressure and reaction products' pressure, respectively; and A, B, R_1, R_2, and ω are adjustable constants.

The chemical reaction rate for the conversion of unreacted explosive to reaction products is:

$$\frac{d\lambda}{dt} = I(1-\lambda)^b\left(\frac{\rho}{\rho_0} - 1 - a\right)^x + G_1(1-\lambda)^c \lambda^d P^y + G_2(1-\lambda)^e \lambda^g P^z \tag{3}$$

where λ is the fraction of the reacted material, t is time, ρ is the current density,

Copyright © 2017 Institute of Industrial Organic Chemistry, Poland

ρ_0 is the initial density, P is the pressure in Mbar, and I, G_1, G_2, a, b, c, d, e, g, x, y, and z are adjustable constants. This three-term model consists of an ignition term and two growth terms.

The parameters of the unreacted JWL EOS were determined by the shock pressure-volume relationships of C-1, which were obtained in previous shock initiation experiments for C-1, using an *in-situ* electromagnetic gauging technique. The initial pressure of the unreacted C-1 explosive is standard atmospheric pressure, which does not change with increasing temperature; thus, the unreacted JWL EOS parameters at different temperatures can be obtained by adjusting the value of the parameter B with changing temperature T_0 [15]. Another parameter that changes with temperature is the explosive density; the change in density is caused by the thermal expansion of C-1 during the heating process. The coefficient of thermal expansion for the ε phase of CL-20 is 0.00014/K in the range of 300-390 K [8]; after the ε→γ phase transition, the volume of C-1 is 6% larger [10]. The JWL EOS parameters of the reaction products were obtained by a cylinder test for the C-1 explosive. In the simulation, the product JWL EOS parameters were assumed to be constant at different temperatures. The unreacted and product JWL EOS parameters for C-1 at different temperatures are listed in Table 3.

The approach for determining the parameters uses a combination of excitation data for LX-19 (95.2 wt.% ε-CL-20, 4.8 wt.% Estane binder) [2], which is also a CL-20 based explosive. The ignition and growth reactive flow model is based on the hot-spot theory: as the C-1 temperature is increased, the density of the specimen decreases, and the porosity increases, leading to the formation of more hot-spot ignition sites under shock compression. The increased shock sensitivity may also be attributed to the more rapid growth of the reacting hot spots because the chemical decomposition is propagating in C-1 that is hotter than C-1 shocked at ambient temperature. The coefficient of thermal expansion for CL-20 is relatively small; thus, the effect of thermal expansion on the ignition term of the reactive flow model is ignored, and only the influence of temperature on the coefficient G_1 is included in the growth term. The values of G_1 at these temperatures are shown in Table 3. The experimental and calculated pressure histories for the shock initiation of C-1 at 48 °C, 75 °C, and 125 °C are shown in Figures 6a, 6b, and 6c, respectively.

Copyright © 2017 Institute of Industrial Organic Chemistry, Poland

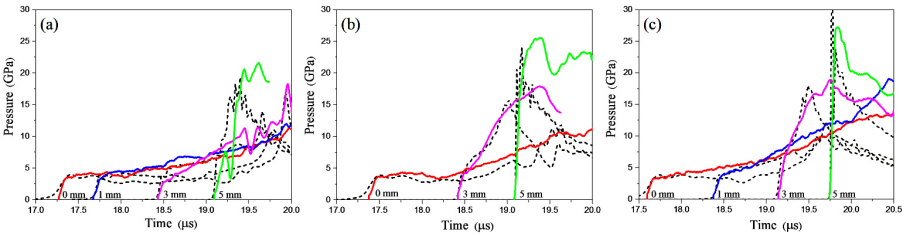

Figure 6. Experimental (solid lines) and calculated (broken lines) pressure histories for shock initiation of C-1 at (a) 48 °C, (b) 75 °C, (c) 125 °C

Table 3. Ignition and growth model parameters for C-1 at various temperatures

Temperature [°C]	Unreacted JWL	Product JWL	Reaction rate parameters	
20	A = 156.825 Mbar	A = 17.918 Mbar	I = 7.43E+11	$G_2 = 400$
	B = −0.3238006 Mbar	B = 1.329 Mbar	a = 0.0	e = 0.333
	$R_1 = 8.944$	$R_1 = 6.2$	b = 0.667	g = 1.0
	$R_2 = 2.464$	$R_2 = 2.85$	x = 20	z = 2.0
	ω = 0.8695	ω = 0.55	$G_1 = 360$	$F_{igmax} = 0.3$
	$C = 2.7814 \times 10^{-5}$ Mbar·K^{-1}	$C = 1.0 \times 10^{-5}$ Mbar·K^{-1}	c = 0.667	$F_{G1max} = 0.5$
	$T_0 = 293$ K	$E_0 = 0.113$ Mbar	d = 0.333	$F_{G2min} = 0.5$
	$\rho_0 = 1.910$ g·cm^{-3}		y = 2.0	
	Shear Modulus = 0.0454 Mbar			
	Yield Strength = 0.002 Mbar			
48	B = −0.3317584 Mbar		$G_1 = 410$	
	$\rho_0 = 1.903$ g·cm^{-3}			
75	B = −0.3394319 Mbar		$G_1 = 460$	
	$\rho_0 = 1.895$ g·cm^{-3}			
95	B = −0.3451161 Mbar		$G_1 = 500$	
	$\rho_0 = 1.890$ g·cm^{-3}			
125	B = −0.3536423 Mbar		$G_1 = 450$	
	$\rho_0 = 1.810$ g·cm^{-3}			
142	B = −0. 3584739 Mbar		$G_1 = 430$	
	$\rho_0 = 1.773$ g·cm^{-3}			
175	B = −0.3678527 Mbar		$G_1 = 580$	
	$\rho_0 = 1.767$ g·cm^{-3}			

Copyright © 2017 Institute of Industrial Organic Chemistry, Poland

The relation between the coefficient G_1 and temperature T is shown in Figure 7. G_1 is 360, 410, 460, and 500 when T equals 20 °C, 48 °C, 75 °C, and 95 °C, respectively. The data show an approximate linear relationship between G_1 and T. This relationship can be described as:

$$G_1 = a + bT \tag{4}$$

where a and b are constants. Based on the simulation results, a and b were obtained using a linear fit; here $a = 321.71$ and $b = 1.86$. Using these values in Equation 4, G_1 at any temperature between 20 °C and 95 °C can be calculated. When the temperature of C-1 is increased to 125 °C, the specimen has partially converted from the ε phase to the γ phase, which leads to a decrease in the reaction rate of C-1, and G_1 decreases to 450. As the temperature of C-1 is increased to 142 °C, the polymorphous transformation of CL-20 from the ε to γ phase is complete and G_1 is further reduced to 430. However, as the temperature is increased further, reaching 175 °C, G_1 increases from 430 to 580. Compared with the increasing trend of G_1 at 20-95 °C, G_1 increases more rapidly with temperature after the ε→γ phase transition of CL-20. Thus, the increasing temperature has a stronger effect on the shock sensitivity of C-1 in the γ phase than in the ε phase.

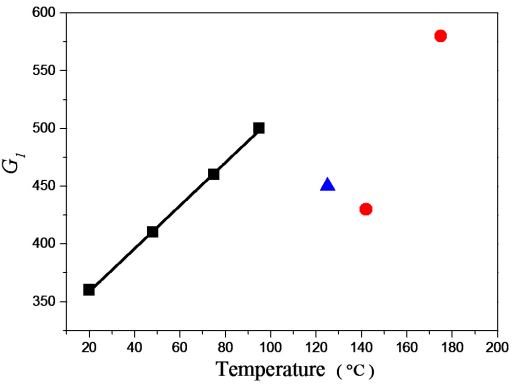

Figure 7. Relation between the coefficient G_1 and temperature T

The distance to detonation as a function of the initial shock pressure, the Pop-plot [16], can reflect the shock sensitivity of the explosive material to some extent. Hence, a flyer impact simulation model was established to calculate the Pop-plot. A plane shock wave is generated by the impact between the flyer plate and the buffer plate; the initial shock pressure can be adjusted by changing the flyer plate velocity. Using the simulation model presented here, the distance to

Copyright © 2017 Institute of Industrial Organic Chemistry, Poland

the detonation point at different initial shock pressures can be calculated. The relative shock sensitivity of C-1 at various initial temperatures is illustrated on the Pop-plot shown in Figure 8. C-1 is most sensitive at 175 °C, followed by 95 °C, 75 °C, 142 °C, 48 °C, and 20 °C in descending order of sensitivity.

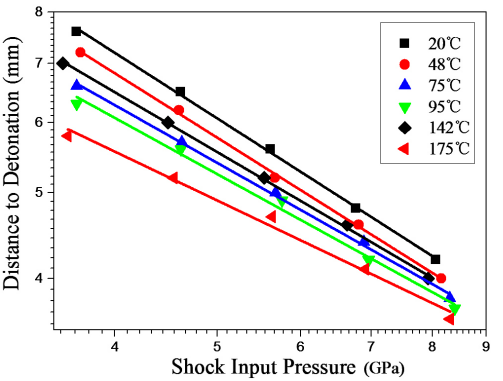

Figure 8. Pop-plot for C-1 at various temperatures

6 Conclusions

To analyze the influence of temperature on the shock sensitivity of CL-20, shock initiation experiments on heated C-1 explosive specimens were performed at various temperatures. Manganin pressure gauges were attached to the specimen to measure the pressure histories at several distances from the impact surface. An ignition and growth reactive flow model was used to simulate the shock initiation of C-1 at different temperatures. The main conclusions are as follows.

C-1 becomes more sensitive as the temperature is increased from 20 °C to 95 °C. The ε to γ phase transition in CL-20 occurs at 125 °C, and C-1 at 142 °C is less shock sensitive than at 95 °C or 75 °C, although the phase transformation causes a volume expansion of the CL-20, which creates more hot spots under shock compression. Thus, the decreased sensitivity of C-1 is due to the γ-phase CL-20 at 142 °C, which is less shock sensitive than the ε-phase CL-20 at 95 °C or 75 °C. When the polymorphic transformation from ε to γ phase in the CL-20 is complete, as the temperature is further increased from 142 °C to 175 °C, the shock sensitivity of C-1 increases again. The simulated results show that the coefficient G_1 in the growth term of the ignition and growth reactive flow model has a linear relationship with the temperature between 20 °C and 95 °C.

The present experimental and simulated results describe the shock initiation

Copyright © 2017 Institute of Industrial Organic Chemistry, Poland

characteristics of C-1 within the temperature range of 20-175 °C. Note that this study only investigated the shock initiation of unconfined heated C-1. Further investigations should focus on the effect of confinement and thermal cycling on the shock initiation of C-1.

Acknowledgments
The authors would like to thank Long Wang, Fu-Ping Wang, De-Shen Geng, Xiao Ma, Kai-Long Xiang, and Ming-Lei Chen for their assistance and support in carrying out this study.

References

[1] Simpson, R. L.; Urtiew, P. A.; Ornellas, D. L.; Moody, G. L.; Scribner, K. J.; Hoffman, D. M. CL-20 Performance Exceeds that of HMX and its Sensitivity is Moderate. *Propellants Explos. Pyrotech.* **1997**, *22*(5): 249-255.
[2] Tarver, C. M.; Simpson, R. L.; Urtiew, P. A. Shock Initiation of an ε-CL-20-Estane Formulation. *Proc. Conf. American Physical Society Topical Group on Shock Compression of Condensed Matter*, AIP Publishing, **1996**, *370*(1): 891-894.
[3] Tarver, C. M.; Forbes, J. W.; Urtiew, P. A.; Garcia F. Shock Sensitivity of LX-04 at 150 °C. In: *Shock Compression of Condensed Matter-1999*, AIP Publishing, **2000**, *505*(1): 891-894.
[4] Urtiew, P. A.; Tarver, C. M.; Maienschein, J. L.; Tao, W. C. Effect of Confinement and Thermal Cycling on the Shock Initiation of LX-17. *Combust. Flame* **1996**, *105*(1): 43-53.
[5] Urtiew, P. A.; Forbes, J. W.; Tarver, C. M.; Vandersall, K. S.; Garcia, F.; Greenwood, D. W.; Maienschein, J. L. Shock Sensitivity of LX-04 Containing Delta Phase HMX at Elevated Temperatures. *AIP Conference Proc.*, IOP Institute of Physics Publishing Ltd., **2004**, *706*(2): 1053-1056.
[6] Russell, T. P.; Miller, P. J.; Piermarini, G. J.; Block, S. High-pressure Phase Transition in Gamma-Hexanitrohexaazaisowurtzitane. *J. Phys. Chem.* **1992**, *96*(13): 5509-5512.
[7] Russell, T. P.; Miller, P. J.; Piermarini, G. J.; Block, S. Pressure/Temperature Phase Diagram of Hexanitrohexaazaisowurtzitane. *J. Phys. Chem.* **1993**, *97*(9): 1993-1997.
[8] Gump, J. C.; Peiris, S. M. Phase Transitions and Isothermal Equations of State of Epsilon Hexanitrohexaazaisowurtzitane (CL-20). *J. Appl. Phys.* **2008**, *104*(8): 083509.
[9] Ma, X. *Research on the Thermal Reaction Characteristics and Rules of High Mixed Explosives*. Beijing Institute of Technology Press, Beijing **2014**, pp. 36-37.
[10] Gustavsen, R. L.;, Gehr R. J.; Bucholtz S. M.; Alcon R. R.; Bartram B. D. Shock

Copyright © 2017 Institute of Industrial Organic Chemistry, Poland

Initiation of the Tri-amino-tri-nitro-benzene Based Explosive PBX 9502 Cooled to 55 °C. *J. Appl. Phys.* **2012**, *112*(7): 74909.

[11] Tian, Q.; Yan, G.; Sun, G.; Huang, C.; Xie, L.; Chen, B.; Huang, M.; Li, H.; Liu, Y.; Wang, J. Thermally Induced Damage in Hexanitrohexaazaisowurtzitane. *Cent. Eur. J. Energ. Mater.* **2013**, *10*: 359.

[12] Hallquist, J. O.; Benson, D. J. *LS-DYNA User's Manual–Nonlinear Dynamic Analysis of Structures in Three Dimensions*. Livermore Software Technology Corporation, California USA **1993**, pp.17.

[13] Lee, E.; Finger, M.; Collins, W. *JWL Equation of State Coefficients for High Explosives*. No. UCID-16189, **1973**.

[14] Tarver, C. M.; Hallquist, J. O.; Erickson, L. M. *Modeling Short Pulse Duration Shock Initiation of Solid Explosives*. No. UCRL-91484, Lawrence Livermore National Lab., CA (USA) **1985**.

[15] Urtiew, P. A.; Vandersall, K. S.; Tarver, C. M.; Garcia, F. *Initiation of Heated PBX-9501 Explosive when Exposed to Dynamic Loading*. No. UCRL-CONF-214667, Lawrence Livermore National Lab., **2005**.

[16] Ramsay, J. B.; Popolato, A. *Analysis of Shock Wave and Initiation Data for Solid Explosives*. No. LA-DC-6992, Los Alamos Scientific Lab., Univ. of California, N. Mex. **1965**.

Copyright © 2017 Institute of Industrial Organic Chemistry, Poland